Research paper

Performance Characterisation of a Separated Heat-Pipe-Heat-Recovery-Heat-Exchanger for the food drying industry

N.S. Thomas* and R.T. Dobson[a]

[a]*Department of Mechanical and Mechatronic Engineering, University of Stellenbosch, Stellenbosch, South Africa*

HIGHLIGHTS

- Heat pipes/thermosyphons can transfer large amounts of energy across large distances
- Correlations are not common for separated HPHE's
- Heat transfer coefficients are predicted to reasonable accuracy
- Numerical program predicts heat transfer to within 12%

ARTICLE INFO

Article info:
Received
Accepted
Available online

Keywords:
Heat recovery
Natural circulation thermosyphon
Heat Pipe Heat Exchanger HPHE
Separated-HPHRHE
Heat transfer coefficients
Waste heat recovery

ABSTRACT

This paper presents the performance evaluation of a separated-HPHRHE for use in the food processing industry. The outside heat transfer coefficients were obtained by passing hot air over a HPHE filled with cold water and of similar geometry to the HPHE's used for the separated-HPHE. The inside heat transfer coefficients for the separated-HPHE were determined with R600a, R134a and R123 as working fluids. The experiments were undertaken at various temperatures and flow rates. The results showed that R600a works the most effectively in the temperature range considered and this is expected since R600a is less dense and has a higher latent heat of vaporisation than both R134a and R123. As an example, the R600a charged separated-HPHE yielded heat transfer rates in the region of 9352 W compared to the 7017 W and 4555 W yielded for R134a and R123 respectively at an air temperature difference of 27 °C and mass flow rate of 0.841 kg/s. The as-tested separated-HPHRHE was shown to have worked effectively (recovering up to 90 % of the of the dryer exhaust heat) for typical food industry drying temperatures of between 25-80 °C. Additionally, the theoretical simulation models for the HPHRHE was validated in as much that its energy saving performance was within ± 12 % of the as-tested experimental models; and thus it was demonstrated that substantial energy cost saving could be realised using standard heat exchanger manufacturing technology. It is recommended that notwithstanding accuracies of roughly 22 % obtained by the theoretically predicted correlations to the experimental work, the heat exchanger design should be optimised to allow better refrigerant flow and various performance parameters such as liquid fill charge ratio and condenser/evaporator length dependencies should be further investigated.

Nomenclature

A	area, m^2
c_p	specific heat, J/kgK
d	diameter, m
h	heat transfer coefficient, W/m^2K
k	thermal conductivity, W/Mk
$\dot{m}$	mass flowrate, kg/s
Ja	Jacob number, $c_{pl}(T_w-T_{sat})/h_{fg}$
Ku	Kutateladze number, $\dot{q}_e\sqrt{\sigma/g(\rho_l-\rho_v)}\,/(\rho_v v_l h_{fg})$
k	thermal conductivity, W/Mk
Pr	Prandtl number, $c_p\mu/\rho$
$\dot{Q}$	heat transfer rate, W
R	thermal resistance, K/W: coefficient of determination
Re	Reynolds number, $\rho V d_h/\mu$
S	pitch, m
T	temperature, °C

Subscripts

air	air
c	cold, condenser
e	evaporator
exp	experimental
f	fin, frontal, fluid
g	gas
h	hot, hydraulic
hp	heat pipe
i	inside
L	longitudinal
m	mass
o	outside
pred	predicted
T	transverse
v	vapour
w	wall

Abbreviations: HPHE, heat pipe heat exchanger; HPHRHE, heat-pipe-heat-recovery-heat-exchanger; ID, internal diameter; OD, outside diameter; VSD, variable speed drive;

* Corresponding author, Tel: +27 21-808-4078
E-mail address: 15818705@sun.ac.za, rtd@sun.ac.za[a]

1. Introduction

As our limited non-renewable energy resources diminish and become more costly, energy conservation and wasteheat utilisation become increasingly important engineering design considerations. Waste heat streams have high energy content which can be utilised elsewhere in athermal process. WHRU's use this waste heat to improve the efficiency of a process. HPHRHE's are one specific type of WHRU which uses heat pipes to transfer heat from the hot exhaust stream to the cooler inlet stream. Heat pipes are essentially natural heat pumps which use the large latent heat of vaporisation of a refrigerant to transfer energy [1]. Heat pipes have the distinct advantage over other WHRU's of being able to transfer large amounts of energy across relatively long distances, which allows the process streams to be separated. This is especially necessary for the food manufacturing industry, where cross contamination is undesired.Additionally, heat pipes are self-contained, essentially fouling and corrosion resistant and have no moving parts and gasket material which could leak. All of these characteristics make heat pipes very suitable for any heat recovery application.

A heat pipe consists of a sealed pipe lined with an internal wicking structure and a hollow inner section, which contains a small amount of working fluid. It consists of two sections, the evaporator and condenser. Heat supplied to the evaporator section by a hot fluid stream heats the working fluid till it vaporises. The pressuredifference between the two sections causes the vapour to flow to the condenser section, where it gives off its latent heat of vaporisation and condenses. The capillary forces in the wicking structure "pump" the fluid back to the evaporator section and the process repeats itself.Heat pipes are very efficient due to the minimal temperature drop between the evaporator and condenser.

Thermosyphons are heat pipes without a wicking structure. The fundamental difference between heat pipes and thermosyphons is that thermosyphons utilise gravity to allow condensate flow back to the evaporator, instead of the capillary forces in the wicking structure of a "normal" heat pipe. Similar to heat pipes, the working fluid is vaporised by heat addition in the evaporator section and the vapour moves into the condenser section due to the pressure difference between the two sections. The working fluid then gives off its latent heat of vaporisation to the cooler condenser section and as such condenses. The condensate runs down the tube wall under the influence of gravity and the process is repeated. Thermosyphons are preferred due to their lower condensate flow resistance. The wicking structure in a heat pipe causes a condensate flow resistance which decreases the attainable heat flux in a heat pipe by 1.2 to 1.5 times below that of a thermosyphon[1]. Furthermore, "normal" heat pipes are moreexpensive to manufacture than thermosyphons because they are structurally more complicated.

Thermosyphons can be used in what is termed a "separated loop"arrangement as shown in Figure 1[2]. [3] successfully illustrated this in the cooling of an electronic cabinet. They found that an energy recovery of up to 500 W is possible using a single 12.7 mm OD separated thermosyphon. The principle of operation remains the same: the working fluid is vaporised in the evaporator section and runs in the vapour line to the condenser, where heat is removed and condensation occurs. Any vapour still present after the condenser is condensed in the liquid line. Here it is imperative that the condenser section be located at a relative position which is above the evaporator section. Consequently, the liquid line must have a net downward gradient toward the evaporator. To minimise flow losses, smooth walls must be employed in the fluid lines.

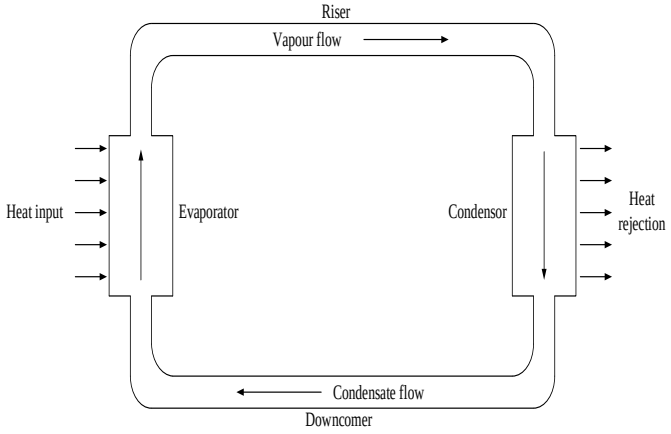

Figure 1 Separated loop thermosyphon

HPHE's are increasing in popularity due to the fact that they are easy to manufacture, cheap to maintain and redundant in their design, i.e, if a row of pipes fail the heat exchanger continues to function. However, thermal performance correlations for separated-HPHE's are not easily found in literature. Thus the main objective of this paper is to evaluate the thermal performance of a separated-HPHRHE using readily obtainable refrigerants specifically for use in the food processing industry.

Successful evaluation of the thermal performance of a separated-HPHE requires that the heat transfer characteristics of the heat exchanger is known. Thus the development of appropriate theoretical outsideand insideheat transfer coefficients for different working fluids based on experimental data is important.The influence of other heat exchanger parameters such as tube diameters, fin spacing andtube configuration are readily available in general heat exchanger literature and are thus not considered in this paper. The refrigerants used in this study are R134a, R600a and R123, due to

the fact that they work well in the desired temperature range (10°C– 80°C) and all of these fluids have low ozone depletion and global warming potentials, which make them valuable for practical applications.

2. Theory

Consider a single thermosyphon and its inputs and outputs as illustrated in Figure 2. Heat is transferred (in the case of the evaporator) from the heat source, through the pipe wall and into the refrigerant inside the thermosyphon. The heat transfer occurs in the opposite direction for the condenser section into the heat sink.

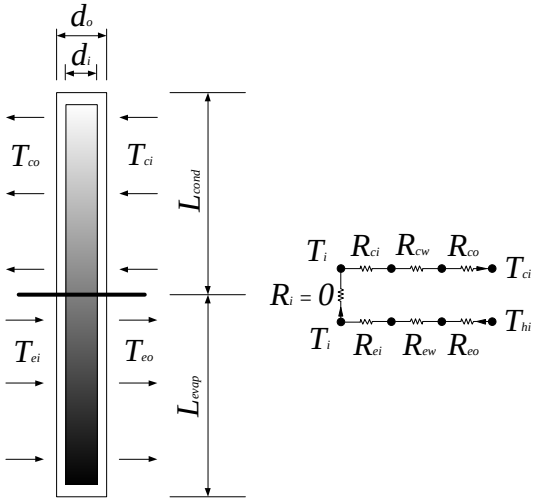

Figure 2 Thermosyphon and thermal resistance diagram

The thermal resistance diagram shown in Figure 2 indicates all the relevant parameters when evaluating the thermal performance of a thermosyphon. These parameters include all the thermal resistances and the temperature differences across these resistances that cause energy/heat to flow in the direction of the negative temperature gradient. Assuming no temperature losses in the thermosyphon along its axial and radial directions, the heat transfer rates of the condenser and evaporator sections can be expressed interms of temperature differences and thermal resistances as

$$\dot{Q}_{hp} = \frac{\bar{T}_h - \bar{T}_c}{\sum R} = \dot{Q}_c = \frac{T_i - \bar{T}_c}{\sum R_c} = \dot{Q}_e = \frac{\bar{T}_h - T_i}{\sum R_e} \quad (1)$$

where

$$\bar{T}_h = \frac{T_{hi}+T_{ho}}{2} \text{and} \bar{T}_c = \frac{T_{co}+T_{ci}}{2}, \quad (2)$$

$$\sum R = \sum R_e + \sum R_c \quad (3)$$

The evaporator and condenser thermal resistances represented in the above equations is a combination of the outside, wall and internal resistance of the thermosyphon and may be expressed as

$$\sum R_e = R_{ei} + R_{ew} + R_{eo}\ , \sum R_c = R_{ci} + R_{cw} + R_{co} \quad (4)$$

with

$$R_{ei} = \frac{1}{h_{ei}A_{ei}},\ R_{ew} = \frac{ln(d_o/d_i)}{2\pi k L_e},\ R_{eo} = \frac{1}{h_{eo}A_{eo}} \quad (5)$$

$$R_{ci} = \frac{1}{h_{ci}A_{ci}},\ R_{cw} = \frac{ln(d_o/d_i)}{2\pi k L_c}, R_{co} = \frac{1}{h_{co}A_{co}} \quad (6)$$

$$A_{ei} = \pi d_i L_e, A_{ci} = \pi d_i L_c,\ A_{eo} = \pi d_o L_e,\ A_{co} = \pi d_o L_c \quad (7)$$

For a row of pipes the respective areas would simply be multiplied by the number of pipes in the row. Knowing the inlet and outlet temperatures and the mass flow rates of the hot and cold streams, the evaporator and condenser section heat transfer rates can be calculated as follows:

$$\dot{Q}_e = \dot{m}_e c_{pair@\bar{T}_h}(T_{hi} - T_{ho}) \quad (8)$$

and

$$\dot{Q}_c = \dot{m}_c c_{pair@\bar{T}_c}(T_{co} - T_{ci}) \quad (9)$$

Once the heat transfer rates of the respective sections are calculated, the inside heat transfer coefficients can be calculated by rearranging equations 1 and 2

$$h_{ei} = \left(A_{ei} \left(\left(\frac{\bar{T}_h - T_i}{\dot{Q}_e} \right) - \frac{1}{h_{eo}A_{eo}} - \frac{\ln\left(\frac{d_0}{d_i}\right)}{2\pi k L_e} \right) \right)^{-1} \quad (10)$$

$$h_{ci} = \left(A_{ci} \left(\left(\frac{T_i - \bar{T}_c}{\dot{Q}_c} \right) - \frac{1}{h_{co}A_{co}} - \frac{\ln\left(\frac{d_0}{d_i}\right)}{2\pi k L_c} \right) \right)^{-1} \quad (11)$$

Knowing the inside working fluid temperature, the wall thermal conductivity and the dimensions of the evaporator and condenser, the respective areas and outside heat transfer coefficients can be calculated. The inside heat transfer coefficients are experimentally determined by using equations 10 and 11.

3. Computer program

A computer program that predicts the performance of the separated-HPHRHE was developed. The inside and outside *h*-values used in the program were determined using correlations found in [4],[5],[6] and [7]. The program uses the geometrical and operating parameters of the heat exchanger as inputs and evaluates whether the specified heat exchanger can provide the required performance. Figure 3 illustrates the operation of the computer program. Table 1 gives the details of the heat exchanger that was specified using the computer program

Table 1 Heat exchanger specifications

Working Fluid	R134a	
Tube material	Copper	
Plate material	Aluminium	
Inlet hot temperature	72	°C
Inlet cold temperature	15	°C
Evaporator and condenser air mass flow rate	0.7	kg/s
Tube bank configuration	Plate-and-tube	

Evaporator and condenser length	0.35	m
Number of tube rows	6	
Number of tubes per row	11	
Longitudinal and transverse pitch	0.0381	m
Fin pitch	10	Fins/in
Fin thickness	0.0002	m
Outside diameter of tubes	0.01588	m
Inside diameter of tubes	0.01490	m

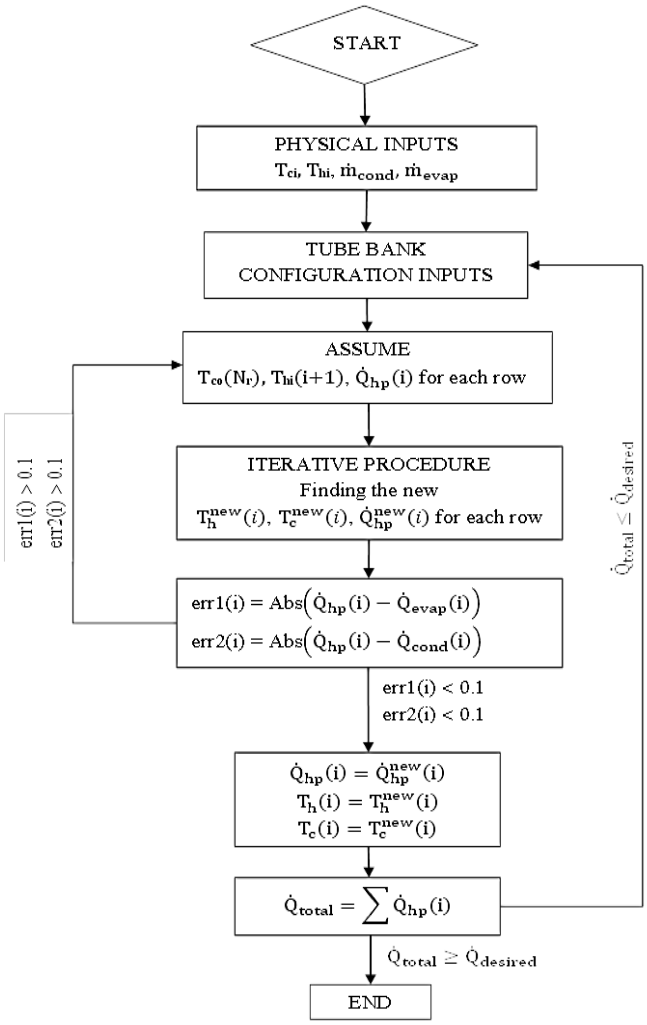

Figure 3 Flow diagram for the computer program

4. Experimental set-up and procedure

To determine the outside heat transfer coefficients, a HPHE of similar geometry to the separated-HPHE with interconnected thermosyphons was used. Cold water from a 2400L supply tank was passed through the HPHE pipes while warm air ranging from 25 °C to 80 °C was drawn through the heat exchanger. The cold water inlet temperature was kept constant by passing it through a chiller in the supply line which kept the water at 5 °C.The mass flow rate of the cold water was determined by filling a 10 L bucketin a given time and measuring the mass of the bucket.To supply a suitable heat input, the radiator was supplied with hot water from a 1800 L supply tank. The water supply setup is shown in Figure 4.

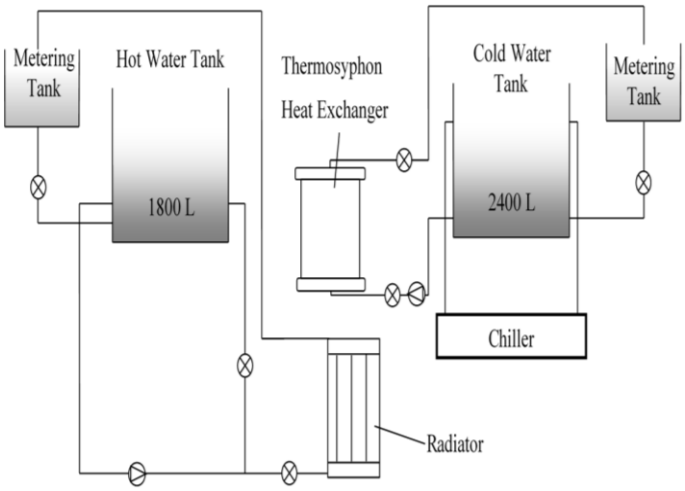

Figure 4Hot and cold water supply

The heat exchanger and radiator were installed in a wooden duct attached to a windtunnel, with the radiator being upstream of the heat exchanger as shown in Figure 5. Temperature measurements at the various points were made every 10 seconds using Type "J" thermocouples and logged using an Agilent 34970A data acquisition unit. Data was measured at various operating conditions for 5 minutes and then the speed of the VSD of the fan is increased in 10 Hz intervals till it reaches 50 Hz. The fan speed is then dropped to 10 Hz and the hot water supply temperature increased and the process is repeated.

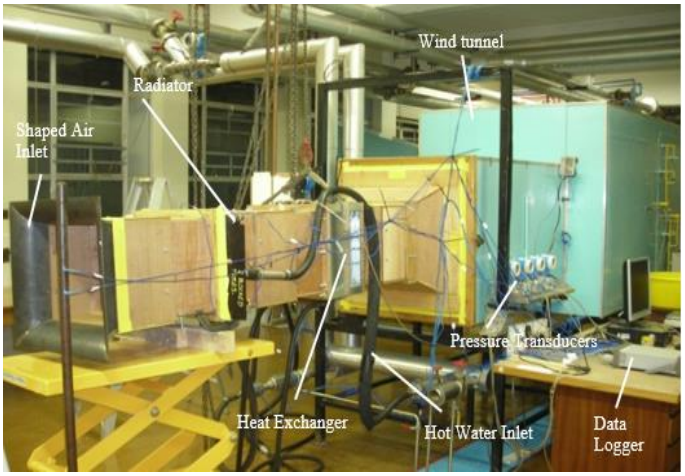

Figure 5Experimental setup for determination of outside *h*-values

The inside heat transfer coefficients were determined in a similar fashion. The separated-HPHE was installed into a modified version of the wooden duct and the evaporator and condenser were connected by copper risers and downcomers which were insulated. The radiator was installed between the two sections, thus the setup represents two different fluid streams as illustrated in Figure 6. The cold water supply was not used for

these experiments. To ensure that the separated-HPHE was vacuum tight, the heat exchanger had to hold a vacuum for at least 5 minutes. It was then charged with refrigerant to 50% of the evaporator volume and "burped" to release any excess air. Air is then drawnthrough the system at various operating conditions and varied in a similar fashion to the outside heat transfer coefficient experiments.

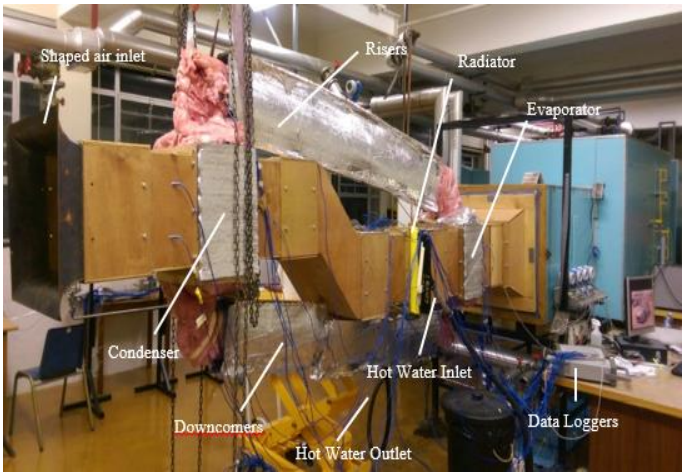

Figure 6Experimental setup for determination of inside*h*-values

5. Results

To correlate the characteristics of the separated-HPHE in terms of independent variables, multi-linear regression techniques were used. The form of the various correlations was chosen to be represented as a power series $= b_n x_1^{c_1} x_2^{c_2} \ldots \ldots$.

5.1 Outside heat transfer coefficients and pressure loss

For these experiments the heat fluxes typically ranged from 7000 W/m^2 – 30000 W/m^2, the air mass flow rates ranged from 0.36 kg/s – 1.2 kg/s and the maximum heat transfer rate reached a value of 34802 W with an average temperature difference of 27.2 °C across the entire heat exchanger. To verify that the data can be used with confidence an energy balance evaluated across the heat exchanger had to be within reasonable limits, as shown in Figure 7.

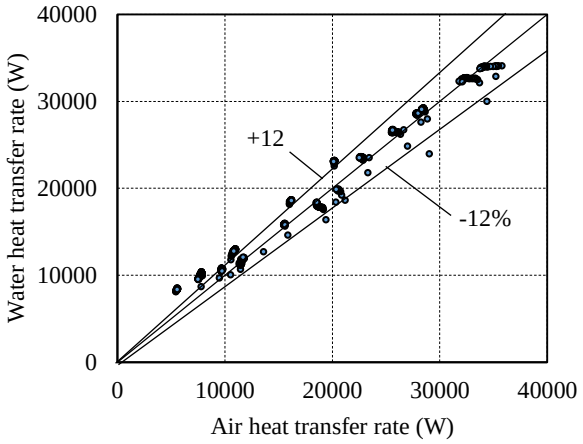

Figure 7Energy balance of the geometrically similar heat exchanger

The results comparing the predicted and experimentally obtained outside *h*-values are shown for each row in Figure 19 in the appendix. The following parameters were identified as the most important independent variables.

$$h_{eo} = f(Re_{air}, Pr_{air}, d_o, S_T, S_L, \ldots\ldots) \quad (12)$$

The Reynolds number captures the air mass flowrate, viscosity and geometric properties of the heat exchanger while the Prandtl number captures the air properties like temperature, specific heat and thermal conductivity. Thus these two variables were used in the multi-linear regression. For row 1 and 2, 95% of the predicted values lie within 5% of the experimental values. For row 3 and 4, 96% of the predicted values fall within 8% and 10% of the experimental values respectively. Row 5 and 6 show alarger scatter in the difference between the predicted and experimental values. For row 5, 90% of the values lie within 11% of each other while for row 6 the values lie within 15% of each other.The outside heat transfer coefficients for each row were determined as follows:

Table 2Row-by-row outside heat transfer coefficients

Row #	Correlation	Correlation coefficient
1	$h_{eo} = 0.00112 Re_{air}^{0.936} Pr_{air}^{-7.562}$	$R^2 = 0.995$
2	$h_{eo} = 0.00254 Re_{air}^{0.839} Pr_{air}^{-8.580}$	$R^2 = 0.988$
3	$h_{eo} = 0.00469 Re_{air}^{0.758} Pr_{air}^{-9.914}$	$R^2 = 0.977$
4	$h_{eo} = 0.00896 Re_{air}^{0.642} Pr_{air}^{-12.401}$	$R^2 = 0.949$
5	$h_{eo} = 0.0168 Re_{air}^{0.463} Pr_{air}^{-17.234}$	$R^2 = 0.995$
6	$h_{eo} = 0.0364 Re_{air}^{0.144} Pr_{air}^{-26.603}$	$R^2 = 0.388$

Figure 8 shows that 94% of the predicted pressure loss values fall within 8% of their experimental counterparts. Similar to the outside heat transfer coefficients, the pressure loss across the heat exchanger is also given in terms of the airside Reynolds and Prandtl numbers.

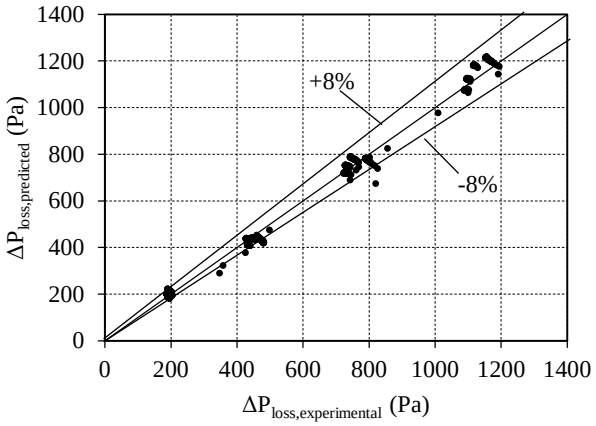

Figure 8Pressure loss across the HPHE

The corresponding pressure loss correlation was obtained as

$$\Delta P_{loss,pred} = 1.210 \times 10^{-6} Re_{air}^{1.583} Pr_{air}^{-5.159} R^2 = 0.972 \quad (13)$$

5.2 Inside heat transfer coefficients

The energy balances for the various refrigerants are shown in Figure 9. These energy balances were deemed acceptable for further data analyses to be done.To correlate the inside *h*-values, the Kutadaledze and Jacob numbers were chosen because they capture the refrigerant and external properties.

With the HPHE filled with R600a, the experimental heat fluxes ranged from 1086 W/m^2 to 13825 W/m^2 and the maximum heat transfer rate obtained 15968 W at an average temperature difference of 38 °C.The experimental correlations are predicted to within 30 % in the worst case for the evaporator as shown in Figures 10 and 11. Considering the chaotic flow takingplace in the evaporator, these predictions were deemed sufficient. The obtained correlations are tabulated below.

Table 3 R600a evaporator inside *h*-value correlations

Row #	Correlation	Correlation coefficient
1	$h_{ei} = 1426.359Ku^{0.261}Ja^{-0.175}$	R^2 = 0.166
2	$h_{ei} = 4776.64Ku^{-0.564}Ja^{0.572}$	R^2 = 0.264
3	$h_{ei} = 2429.97Ku^{-0.414}Ja^{0.182}$	R^2 = 0.398
4	$h_{ei} = 2611.49Ku^{-0.361}Ja^{0.155}$	R^2 = 0.558
5	$h_{ei} = 362.51Ku^{0.84}Ja^{-0.903}$	R^2 = 0.532
6	$h_{ei} = 61.26Ku^{1.732}Ja^{-1.690}$	R^2 = 0.765

The comparison between the predicted inside condenser *h*-values and the experimental results show that the predicted values show a 20% maximum scatter around the experimental values obtained *h*-values are shown in Figures10 and 11. The correlations are tabulated below.

Table 4 R600a condenser inside *h*-value correlations

Row #	Correlation	Correlation coefficient
1	$h_{ci} = 9.415Re^{0.923}(\rho_v/\rho_l)^{1.005}$	R^2 = 0.982
2	$h_{ci} = 1.425Re^{1.069}(\rho_v/\rho_l)^{1.484}$	R^2 = 0.954
3	$h_{ci} = 1097.46Re^{0.762}(\rho_v/\rho_l)^{-0.125}$	R^2 = 0.919
4	$h_{ci} = 1001.249Re^{0.715}(\rho_v/\rho_l)^{-0.118}$	R^2 = 0.917
5	$h_{ci} = 68.246Re^{1.001}(\rho_v/\rho_l)^{0.419}$	R^2 = 0.999
6	$h_{ci} = 14370.66Re^{0.480}(\rho_v/\rho_l)^{-0.802}$	R^2 = 0.963

The results for the case whenthe HPHE was filled with R134a are shown in Figures12and 13 .The heat fluxes for the experiments ranged from 704 W/m^2 – 9694 W/m^2 and the maximum heat transfer rate was obtained as 11763 W at a temperature difference of 40 °C. The correlations obtained from the data analysis are given below for the evaporator. The experimental data was predicted to within 16 %, with only the first evaporator row having an accuracy of 35 %. This is attributed to the large heat flux causing a higher state of disorder in the flow and the evaporator heat transfer coefficients remaining relatively constant.

The correlations obtained for the inside *h*-values are as follows:

Table 5R134a evaporator inside *h*-value correlations

Row #	Correlation	Correlation coefficient
1	$h_{ei} = 6350.69Ku^{-1.826}Ja^{1.994}$	R^2 = 0.549
2	$h_{ei} = 509.276Ku^{0.194}Ja^{-0.268}$	R^2 = 0.237
3	$h_{ei} = 1085.759Ku^{0.019}Ja^{0.076}$	R^2 = 0.095
4	$h_{ei} = 479.191Ku^{0.691}Ja^{-0.574}$	R^2 = 0.654
5	$h_{ei} = 210.364Ku^{1.089}Ja^{-1.137}$	R^2 = 0.693
6	$h_{ei} = 120.069Ku^{1.496}Ja^{-1.507}$	R^2 = 0.966

The comparison between the predicted and experimental condenser inside *h*-values are illustrated in Figures 12 and 13. The experimental values are predicted to within 12%. The correlations are given in Table 6

Table 6R134acondenser inside *h*-value correlations

Row #	Correlation	Correlation coefficient
1	$h_{ci} = 1.998Re^{0.789}\left(\rho_v/\rho_l\right)^{1.376}$	$R^2 = 0.973$
2	$h_{ci} = 7577.68Re^{0.058}\left(\rho_v/\rho_l\right)^{-1.035}$	$R^2 = 0.978$
3	$h_{ci} = 5.026Re^{0.755}\left(\rho_v/\rho_l\right)^{1.126}$	$R^2 = 0.979$
4	$h_{ci} = 101.0105Re^{0.667}\left(\rho_v/\rho_l\right)^{0.272}$	$R^2 = 0.972$
5	$h_{ci} = 5402.139Re^{0.606}\left(\rho_v/\rho_l\right)^{-0.952}$	$R^2 = 0.979$
6	$h_{ci} = 118903.04Re^{0.516}\left(\rho_v/\rho_l\right)^{-1.87}$	$R^2 = 0.968$

Low correlation coefficients were once again obtained for the evaporator section of the HPHE. The evaporator inside *h*-values again stayed relatively constant.

The correlations obtained for R123 are shown in Table 7 and 8. The predicted values in this case did not predict the experimental values well. R123 is the heaviest of the refrigerants, and requires a larger heat flux to function properly. It is clear from the results that R123 was not functioning efficiently at lower temperature differences. The correlations are as follows.

Table 7 R123 evaporator inside *h*-value correlations

Row #	Correlation	Correlation coefficient
1	$h_{ei} = 4999.877Ku^{0.704}Ja^{0.564}$	$R^2 = 0.951$
2	$h_{ei} = 65424.29Ku^{0.455}Ja^{1.407}$	$R^2 = 0.812$
3	$h_{ei} = 1026.09Ku^{-0.257}Ja^{1.143}$	$R^2 = 0.963$
4	$h_{ei} = 557.87Ku^{1.147}Ja^{-0.495}$	$R^2 = 0.964$
5	$h_{ei} = 212.882Ku^{1.180}Ja^{-0.781}$	$R^2 = 0.984$
6	$h_{ei} = 59.79Ku^{1.230}Ja^{-1.168}$	$R^2 = 0.997$

Table 8 R123 condenser inside *h*-value correlations

Row #	Correlation	Correlation coefficient
1	$h_{ci} = 1686.29Re^{0.459}\left(\rho_v/\rho_l\right)^{-0.478}$	$R^2 = 0.758$
2	$h_{ci} = 11553.34Re^{0.409}\left(\rho_v/\rho_l\right)^{-0.873}$	$R^2 = 0.798$
3	$h_{ci} = 19371.23Re^{0.406}\left(\rho_v/\rho_l\right)^{-0.959}$	$R^2 = 0.781$
4	$h_{ci} = 16156.89Re^{0.433}\left(\rho_v/\rho_l\right)^{-0.967}$	$R^2 = 0.758$
5	$h_{ci} = 56467942.58Re^{0.17}\left(\rho_v/\rho_l\right)^{-2.49}$	$R^2 = 0.834$
6	$h_{ci} = 1.879 \times 10^{17}Re^{0.923}\left(\rho_v/\rho_l\right)^{1.01}$	$R^2 = 0.939$

5.3 Performance comparison of different refrigerants

R600a and R134a require small average temperature differences – 10 °C – to function. R123 on the other hand only starts functioning properly from temperature differences of approximately 20 °C. This is expected since it is denser than the other refrigerants and thus will require a larger heat flux to reach the condenser. The results also indicate that when R123 starts working the heat recovered per unit average temperature difference is higher than both R600a and R134a, which indicates that for this geometry and application it is better suited to higher temperature differences. The results are shown in Figure 16 - 18 in the appendix.

6. Discussion and conclusions

The primary focal point of the study was to investigate the thermal performance of a separated-HPHRHE at temperatures encountered in the food drying industry using commonly encountered refrigerants and whether the separated-HPHRHE would yield substantial dividends if installed.

To accurately predict the thermal performance of a separated-HPHE, the outside and inside heat transfer coefficients need to be known.The outside heat transfer properties were investigated by running cold water through a heat exchanger of similar outside geometry to those used for the separated-HPHE and passing hot air over the heat exchanger. The predicted outside heat transfer coefficients matched the experimental data well and can thus be used with confidence for a heat exchanger of a similar geometry as defined in Section 3, Table 1. Typical scatter about the reference line was in the order of 5-15 %.

The inside heat transfer coefficient of many working fluids in different pipe diameters can be modelled by existing correlations [3],[4], [13], but these correlations do not model the common refrigerants used in this study accurately enough. Additionally, the two phase flow is difficult to model due to its chaotic nature and no literature exists on the use of common refrigerants in separated-HPHE's. Thus the inside heat transfer coefficients were determined experimentally.

To evaluate the performance of the different refrigerants and develop evaporator and condenser inside heat transfer coefficients, the separated-HPHE was charged to a fill charge ratio of 50 % of the evaporator length with the respective working fluid in each loop. The heat flux for the experiments ranged from 700-16000 W/m^2. To verify that the separated-HPHRHE was indeed working, the energy balances were first evaluated and these yielded values in the range of 8-13 % across the entire range of experiments and thus the measurements were deemed satisfactory for further data manipulation.

As noted in Section 5.3, the performance of the HPHE is greatly influenced by the working fluid. For similar temperature differences and mass flow rates, R600a and R134a work well even with relatively small temperature differences, but R123 is working very poorly the same stage. The reason for this is attributed to the density of R123 vapour in combination with its high latent heat of vaporisation. Compared to relatively small densities of R600a (0.00251 g/cm^3) and R134a (0.00425 g/cm^3), R123 has a rather high density of 1.4368 g/cm^3. In a separated-HPHE arrangement, the evaporator and condenser are separated by a finite distance which the vapour must first travel before condensing and releasing its large latent heat of vaporisation. Additionally, the vapour must travel upward and has to contend with gravitational effects. Hence, because the gas is heavier, it requires a larger driving force (heat input) to reach the condenser section. The high latent heat required to boil the R123 also means a higher heat input is needed for proper operation. However, at higher temperature differences, it is observed that the heat recovered per unit temperature difference for R123 is higher than both R600a and R134a. This indicates that where there is a higher temperature difference, R123 should work as well as if not better than the other options considered in this study.

The separated-HPHE arrangement was also used to determine the inside heat transfer coefficients of the heat exchanger with different working fluids. The physical behaviour was modelled by equations correlating all the working fluid properties. For the evaporator inside heat transfer coefficients, the dimensionless Kutateladze and Jacob numbers were used because they involve all the properties of interest (density and latent heat of vaporisation for example). The predicted *h*-values were generated by using multi-linear regression techniques. With R600a as refrigerant, it was found that the *h*-values correlate the experimental *h*-values between 10-30 %. Considering the chaotic two phase flow phenomena, the poor manifold header design (which impacts on vapour flow) and the long distance the refrigerant has to transverse to reach the condenser and be effective, the *h*-values' error was acceptable. However, the multi-linear regression yielded low correlation coefficients (R^2). These low correlation coefficients are as a result of the evaporator inside heat transfer coefficients staying relatively constant (see Figures 10 and 11, Appendix A). A suggestion is that for better R^2 values to be obtained, the *h*-values could possibly be formulated with a power series expansion containing more variables. The predicted condenser inside heat transfer coefficients correlate to the experimental *h*-values between 10-25 %. For the condenser inside heat transfer coefficients, the dimensionless numbers used are the Reynolds number and a ratio of the liquid density to the vapour density of the refrigerant. These correlations also yielded high R^2 values, and thus can be used with confidence.

R134a exhibited similar behaviour to R600a. The predicted evaporator *h*-values correlate the experimental *h*-values between 8-35 % and have low R^2 values. It is again observed that the evaporator *h*-values stay relatively constant (Figures 12 and 13). The condenser inside heat transfer coefficients correlate the experimental values to between 10-16 % and have high R^2 values and can thus be used with confidence.

The predicted *h*-values were not correlated well with the experimental *h*-values for R123. Figure 14 and 15 indicate that the predicted evaporator *h*-values correlate the experimental evaporator *h*-values to between 10-33 %. However the R^2 values are high. The predicted condenser inside heat transfer coefficient values correlated the experimental inside heat transfer coefficient values to between 30-40 % with relatively good R^2 values. The primary reason for the scatter in the data is the fact that R123 is not working properly at low temperature differences, as seen in Figure 18 This would yield very low *h*-values. On the other end of the spectrum, the fact that when the heat exchanger is working, the heavy gas coupled with the heavy liquid blasting up and down in the evaporator could cause some scatter in the *h*-values.

Comparable to the experimental results, the numerical simulation predicted similar values for achievable heat transfer rates. Thus the simulation program can be used with confidence. The values were slightly less due to the fact that the program uses empirically calculated values to find the heat transfer resistances, but the heat transfer rates are predicted to within 12 % and is deemed sufficient. The only problem occurs at the low temperature end of R123, where the program does not take into account that the R123 is not working. The theoretical correlations presented in [1] and [4] do not correspond well with the values obtained for the separated-HPHE. This is largely attributed to the fact that the researchers obtained their results by evaluating a single thermosyphon, whereas this study utilised the entire heat exchanger. Thus, while the behaviour of the working fluid was not as carefully controlled in this study, the correlations obtained were used in the numerical program and yielded predictions within an acceptable range, as mentioned above. The insights gained from this study can thus be justified.

While the separated-HPHRHE was not installed in an actual drying application to verify the actual savings and operation, it is clear that there are substantial financial savings to be realized by utilising such a heat exchanger. Even in the worst case scenario the payback period of the heat exchanger unit would not exceed 3 years.

The main objective of the study was met in as much as that the as-tested separated-HPHRHE was shown to worked effectively (recovering up to 90 % of the of the dryer exhaust heat) for typical food industry drying temperatures of between 25 and 80 °C. Furthermore, the theoretical simulation models for the HPHRHE was validated in as much that its energy saving performance was within ± 12 % of the as-tested experimental models; and thus it was demonstrated that substantial energy cost saving could be realised using standard heat exchanger manufacturing technology, but in a novel application. Hence it is recommended that more and more use needs to be made of HPHRHE technology.

7. Recommendations

The following recommendations are provided:

1. The heat exchanger design was not an express objective of this thesis and as such there could not be optimal flow of the refrigerant in each thermosyphon loop. It is recommended that the manifold and geometric design of the heat exchanger be optimised for better refrigerant flow. Also, the effect of these various changes have to be investigated.
2. It was found that if the working fluid is very dense (as is the case with R123), the distance between the evaporator and the condenser plays a vital role in the operation of a separated-HPHRHE. Thus it is recommended that the relationship between heat input and the distance between the two sections be investigated.
3. Each loop in the separated-HPHRHE was filled with a charge fill ratio of 50% of the evaporator volume. For effective low temperature operation this could be a limiting factor because of the amount of energy that must be added to boil off the vapour. Thus a separated-HPHRHE should be investigated with different charge fill ratios.
4. While the inside heat transfer coefficients were determined to reasonable accuracy, they would be better still if a single thermosyphon was considered. The single thermosyphon could then be filled with a variety of common refrigerants (R502, R417, R600a et cetera) to establish which working fluid is best suited to a specific temperature range.
5. The computer program should be made user friendly for use in industry. Subject to the determination of the inside heat transfer coefficients as per Recommendation 4, the program may be used with confidence to develop a range of separated-HPHRHE's.
6. A computational fluid dynamics (CFD) analysis must be done to better understand the boiling characteristics and investigate the inside heat transfer coefficients. Also to investigate the flow of the gas in the riser tube and the look into sufficient riser tube design requirements.
7. For lower temperature applications, the refrigerant used should have a combination of a relatively low latent heat of vaporisation and a gaseous state that is not very dense at the application temperatures. For higher temperatures, heavier working fluids may be considered as the heat input will easily overcome the latent heat of vaporisation. The selection of refrigerants should thus be carefully coupled to these properties.

References

[1] Pioro, L.S. & Pioro, I.L. 1997. *Industrial two-phase thermosyphons*. Begell House

[2] Yun, J. & Kroliczek, E. 2002. Operation of capillary pumped loops and loop heat pipes. *Cooling zone online magazine* 2.6

[3] Dobson, R.T. & Jeggels, Y.U. 2008. Cooling of Electronic Equipment using Bent and Closed Loop Two-phase Thermosyphons, *9th International Heat Pipe Symposium*, Kuala Lumpur, Malaysia

[4] Faghri, A.1995. *Heat pipe science and technology*. Taylor & Francis

[5] Churchill, S.W. & Bernstein, M. 1977. A Correlating Equation for Forced Convection from Gases and Liquids to a Circular Cylinder in Cross Flow. *International Journal ofHeat Transfer* 99: 300-306.

[6] Whalley P.B. 1987. *Boiling, Condensation, and Gas-Liquid Flow*, Clarendon Press, Oxford

[7] Webb, R.L. 1994. *Principles of enhanced heat transfer*, John Wiley

[8] Dobson, R.T. & Kritzinger, O.O. 2008. Electronic Equipment Cabinet Cooling Enhancement using a Two-phase Thermosyphon with Separated Evaporator and Condenser sections, *9thInternational Heat Pipe Symposium*, Kuala Lumpur, Malaysia

[9] Dobson, R. T. & Kröger, D. G. 2000. Thermal characterisation of an ammonia-charged two-phase closed thermosyphon.*R & D Journal* 16.2: 33-40

[10] Dobson, R.T. & Meyer, A. 2006. Thermal Performance Characterization of R134a and Butane Charged Two-Phase Closed Thermosyphons. *R & D Journal* 22.3

[11] Dobson, R.T. & Pakkies, S.A.2002.Development of a heat pipe (two-phased closed thermosyphons) heat recovery heat exchanger for a spray drier. *Journal of Energy in Southern Africa* 13.4

[12] Dobson, R.T. 2006. Energy Saving using Heat Pipe Heat Recovery Heat Exchangers. *South African Energy Efficiency Convention (SAEEC).* Gauteng, South Africa

[13] Dunn, D.P. & Reay, D. 1994. *Heat pipes*, 4th Edition, Pergamon

[14]Emani, M.R.S. 2012. Mathematical Modelling of Thermosyphon Heat Exchanger for Energy Saving. *The Journal of Mathematics and Computer Science* 5.4: 271-279

[15]Kröger, D.G. 1998. *Air-cooled heat exchangers and cooling towers*. Department of Mechanical Engineering, University of Stellenbosch

[16]Lukitobudi. A.R., Akbarzadeh, A., Johnson, P.W. & Hendy, P. 1995. Design, construction and testing of a thermosyphon heat exchanger for medium temperature heat recovery in bakeries. *Heat Recovery Systems and CHP* 15.5: 481-491

[17]Meyer, A. 2003. *Development of a range of air-air HPHRHE*. Master's Thesis. Stellenbosch: University of Stellenbosch

[18]Nuntaphan, A., Tiansuwan, J. & Kiatsiriroat, T. 2002. Enhancement of heat transport in thermosyphons air preheater at high temperature with binary working fluid: A case study of TEG-water. *Applied Thermal Engineering* 22:251-266

[19]Park, Y.J., Kim, C.J. & Kang, H.K. 2002. Heat transfer characteristics of a two-phased closed thermosyphon to the fill charge ratio. *International Journal of Heat and Mass Transfer* 45: 4655-4661

[20]Payakaruk T, Terdtoon P, Ritthidech S. 2000. Correlations to predict heat transfer characteristics of an inclined closed two phase thermosyphon at normal operating conditions, *Applied Thermal Engineering* 20: 781-790

[21]Peterson, G.P. 1994. *An introduction to heat pipes – modelling, testing and applications*, John Wiley and Sons

[22]Pieters, W.H. 2006. Heat pipe heat exchanger technology – saves energy with bottom line benefits, *Mechanical Technology*, July: 4-5

[23]Russwurm A.E. 1980. Q-pipes add a new dimension to waste heat recovery, Part 1,*Heating, Air Conditioning & Refrigeration (Now Refrigeration and Airconditioning.* January: 27-39

APPENDIX A: The Results

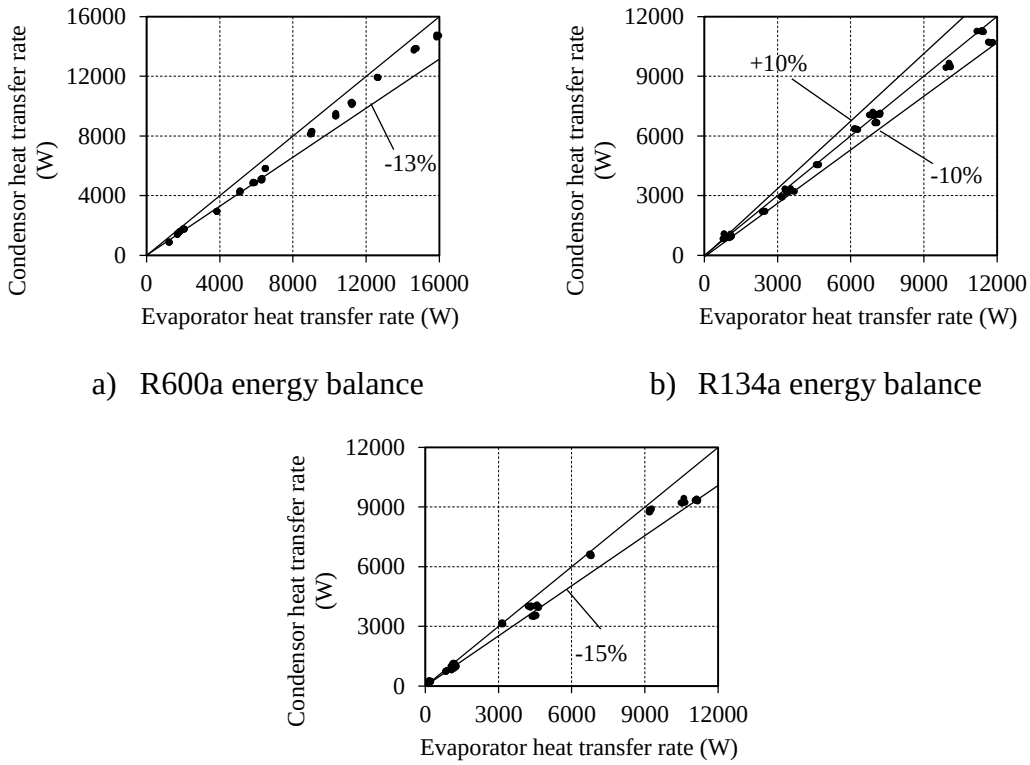

a) R600a energy balance

b) R134a energy balance

c) R123 energy balance

Figure 9 Energy balance of the separated-HPHE operating withR600a, R134a and R123

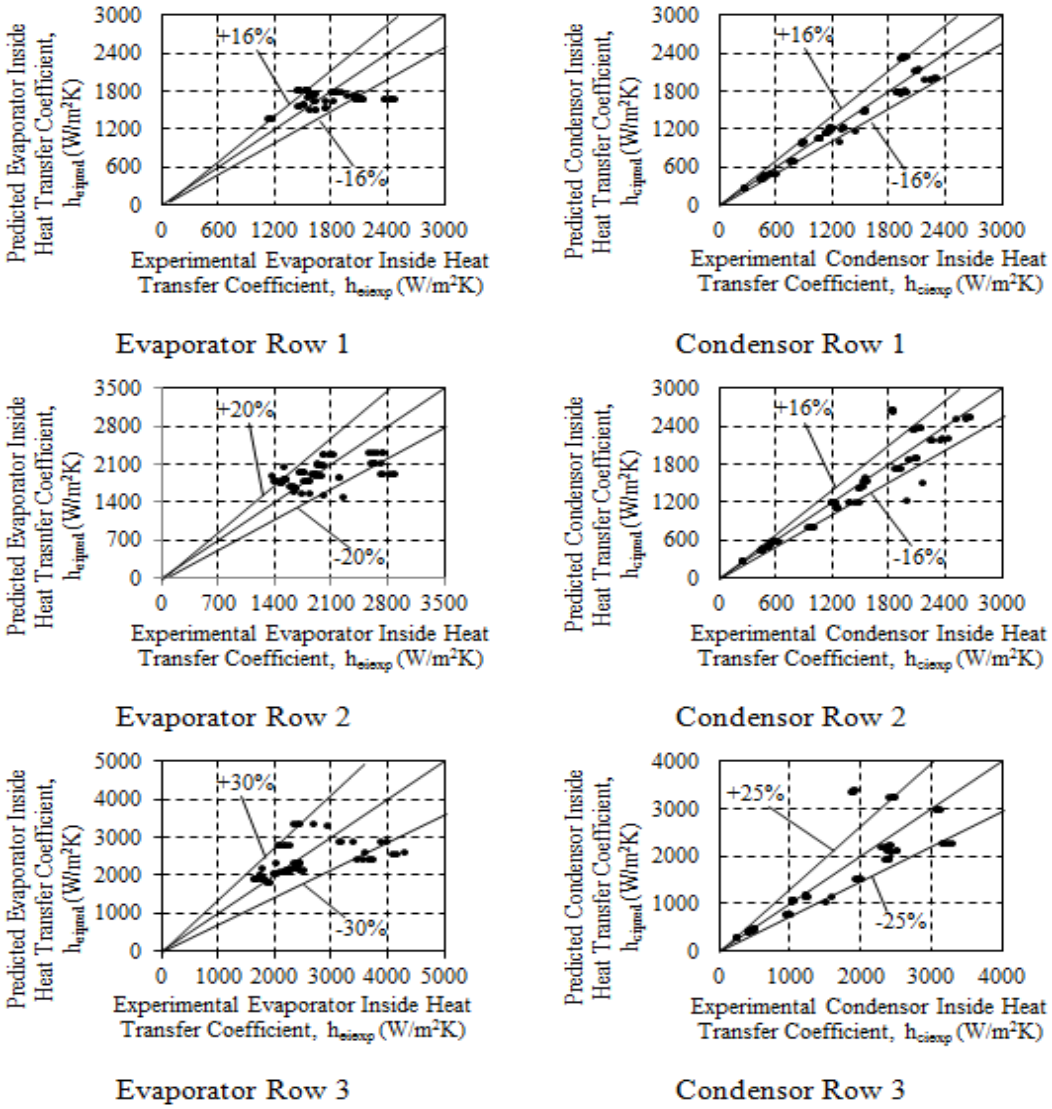

Figure 10 Inside heat transfer coefficients for the separated-HPHE operating with R600a and charged to 50% of the evaporator length for Row 1-3

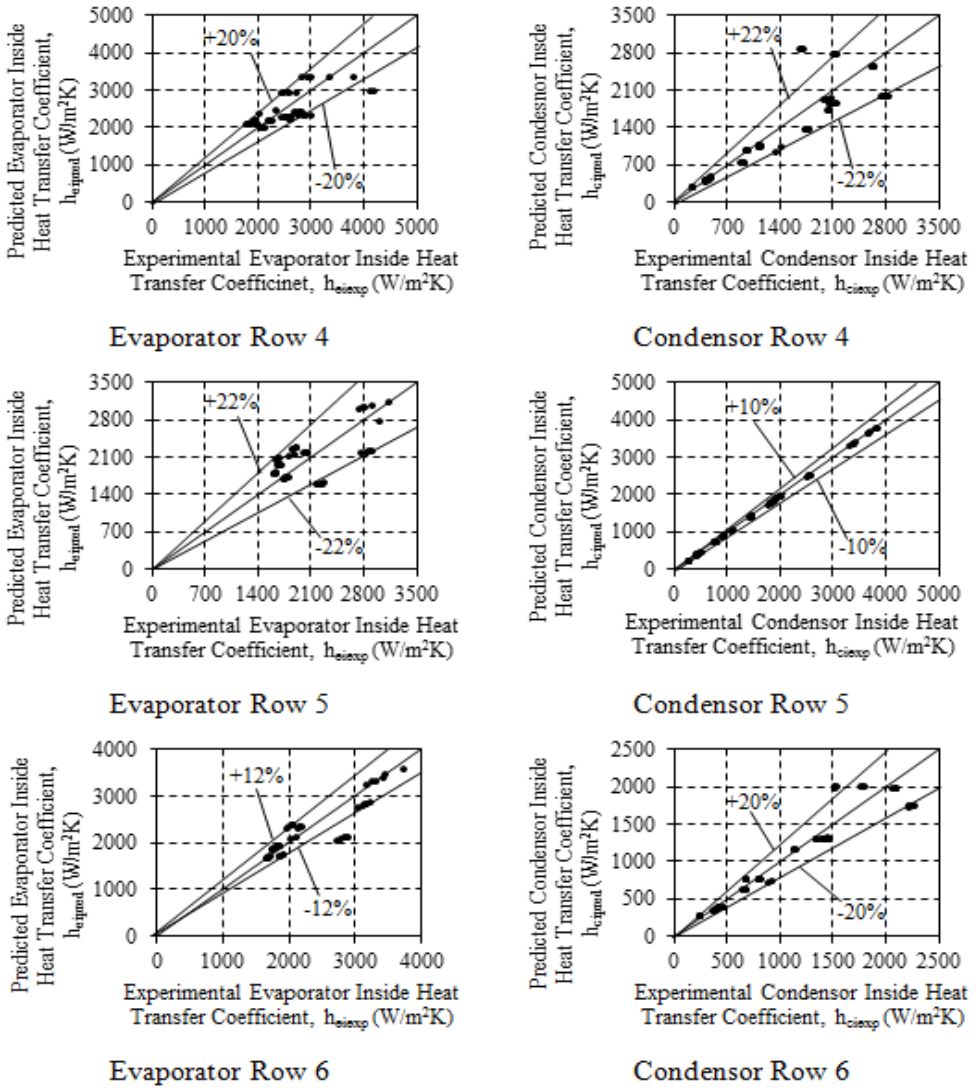

Figure 11 Inside heat transfer coefficients for the separated-HPHE operating with R600a and charged to 50% of the evaporator length for Row 4-6

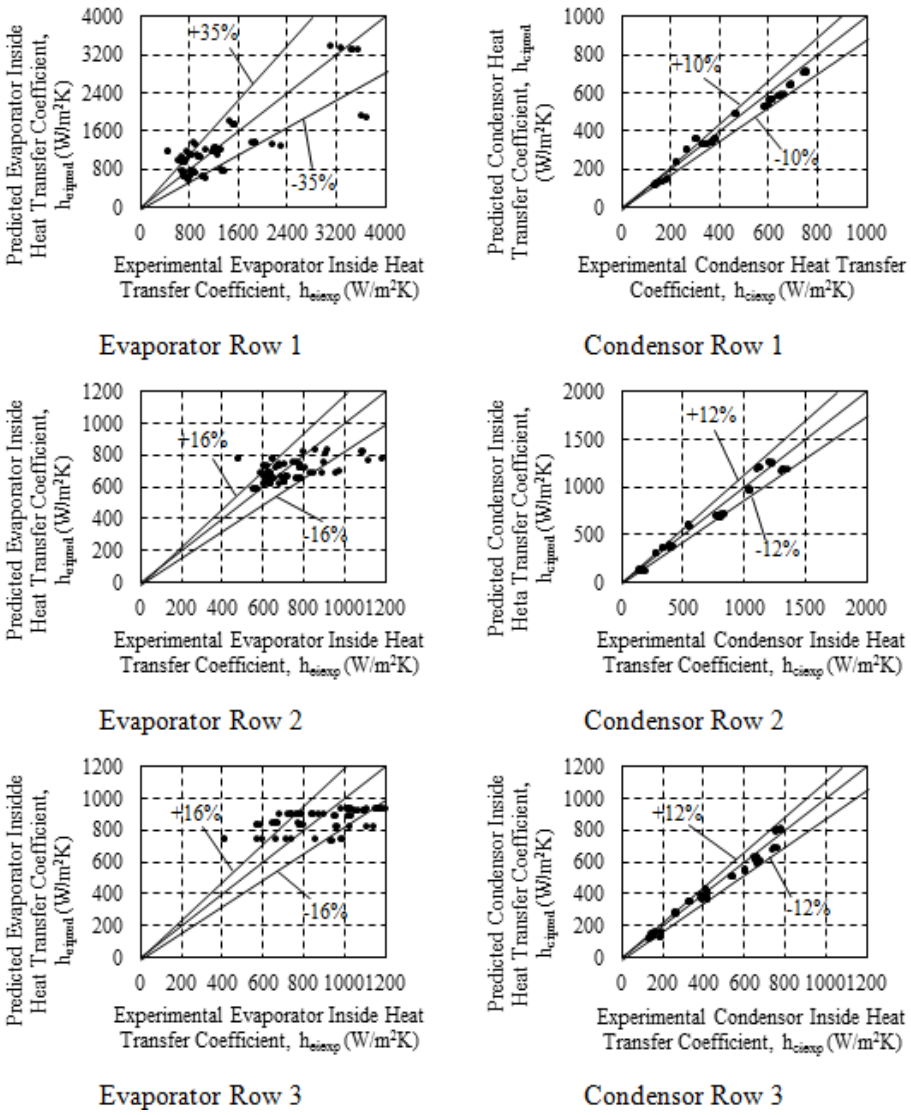

Figure 12Inside heat transfer coefficients for the separated-HPHE operating with R134a and charged to 50% of the evaporator length for Row 1-3

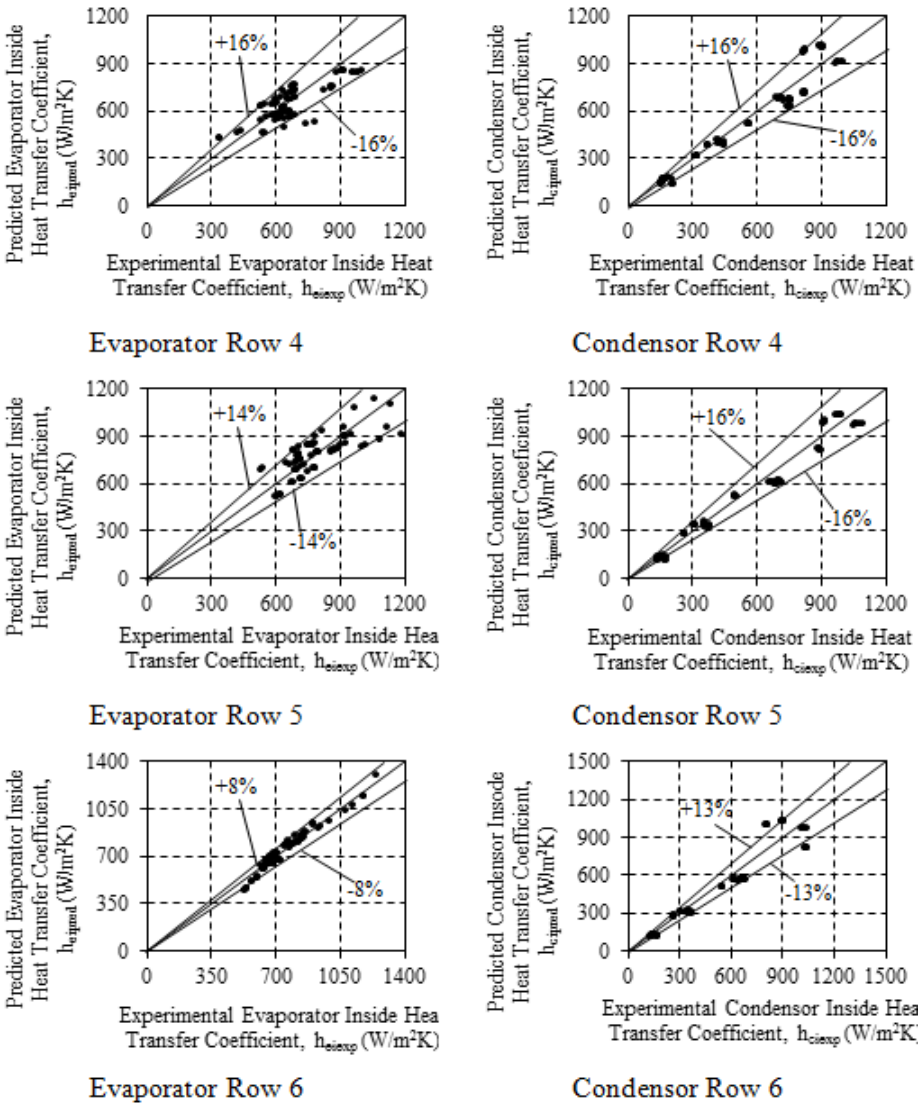

Figure 13 Inside heat transfer coefficients for the separated-HPHE operating with R134a and charged to 50% of the evaporator length for Row 4-6

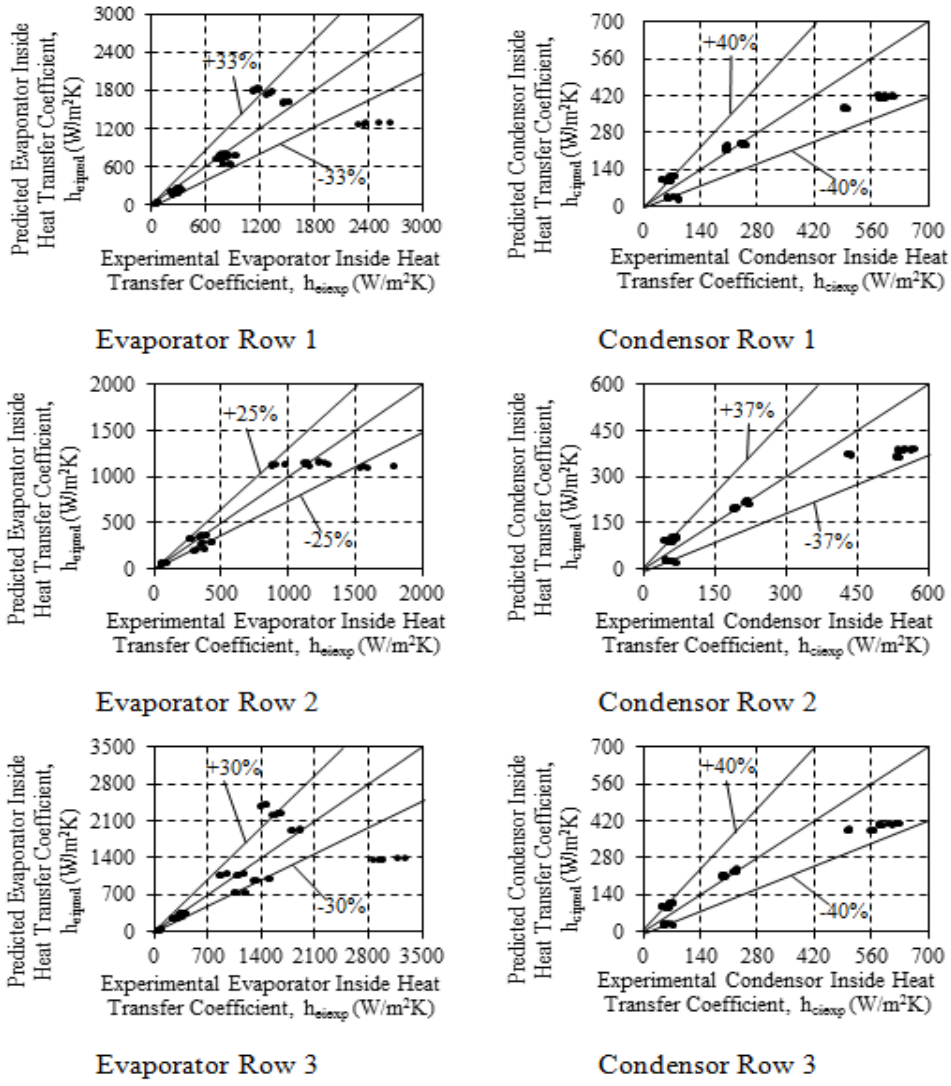

Figure 14 Inside heat transfer coefficients for the separated-HPHE operating with R123 and charged to 50% of the evaporator length for Row 1-3

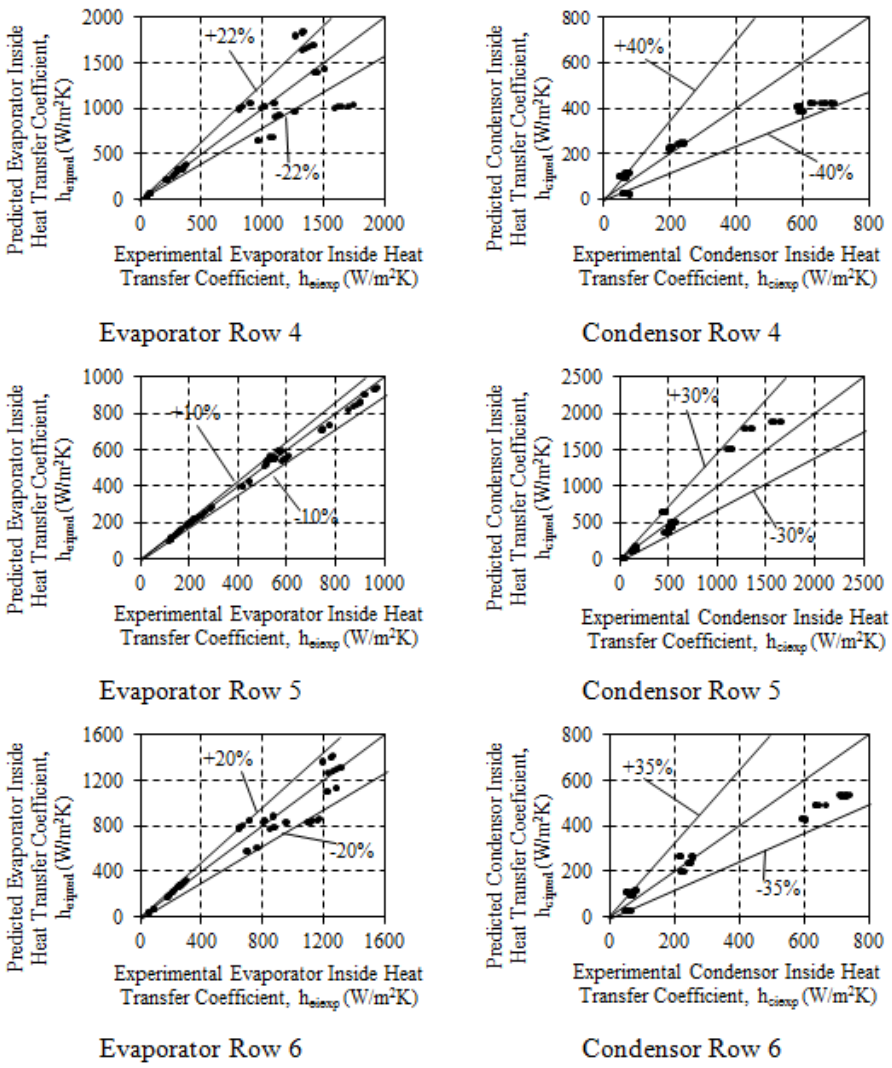

Figure 15 Inside heat transfer coefficients for the separated-HPHE operating with R123 and charged to 50% of the evaporator length for Row 4-6

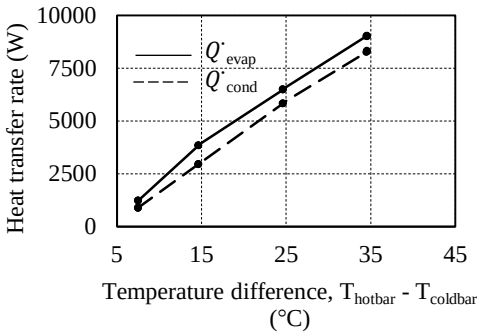

a) $\dot{m}_{air} = 0.374$ kg/s

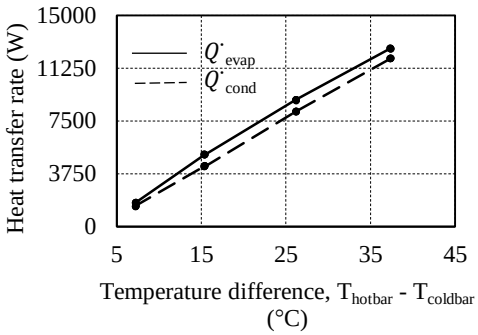

b) $\dot{m}_{air} = 0.579$ kg/s

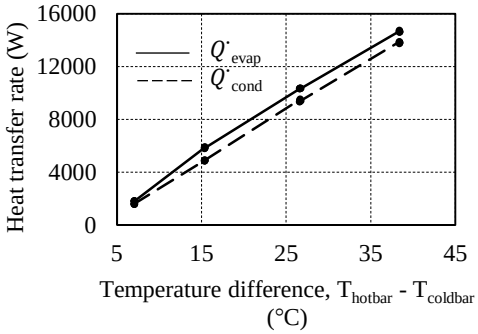

c) $\dot{m}_{air} = 0.841$ kg/s

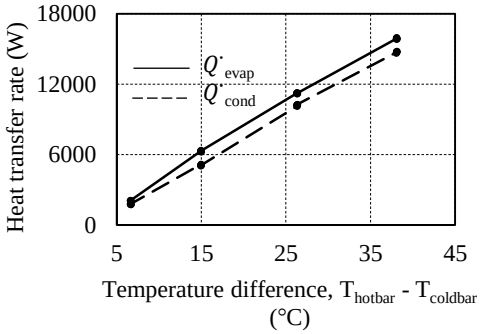

d) $\dot{m}_{air} = 1.112$ kg/s

Figure 16 Thermal resistance curve of the separated-HPHE charged with R600a

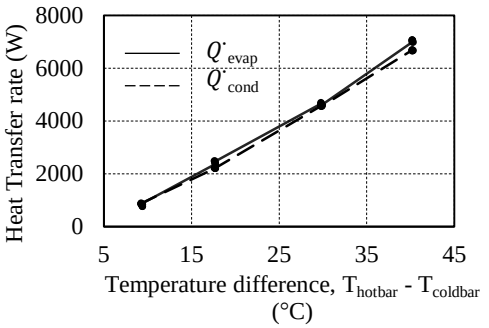

a) $\dot{m}_{air} = 0.374$ kg/s

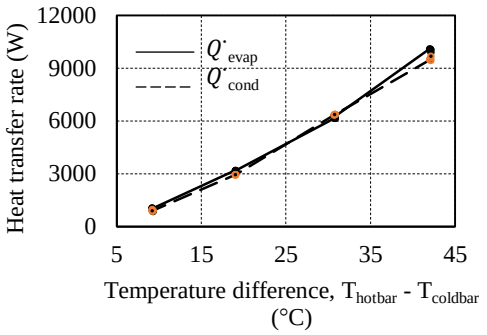

b) $\dot{m}_{air} = 0.579$ kg/s

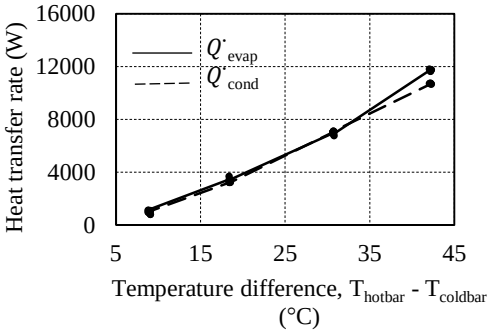

c) $\dot{m}_{air} = 0.841$ kg/s

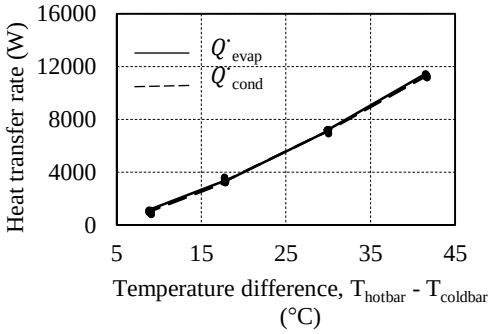

d) $\dot{m}_{air} = 1.112$ kg/s

Figure 17 Thermal resistance curve of the separated-HPHE charged with R134a

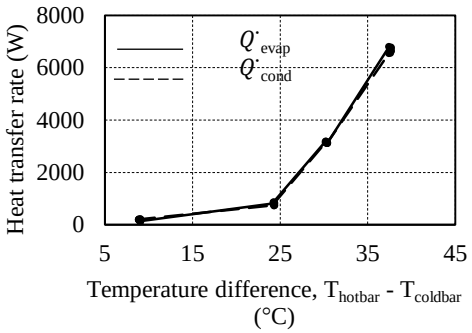

a) $\dot{m}_{air} = 0.374$ kg/s

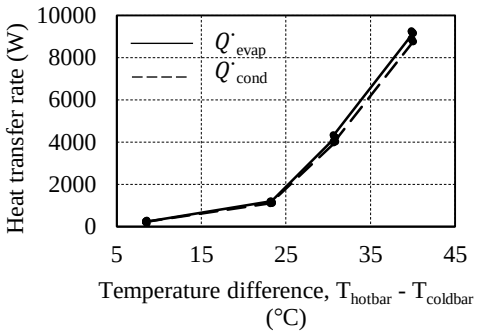

b) $\dot{m}_{air} = 0.579$ kg/s

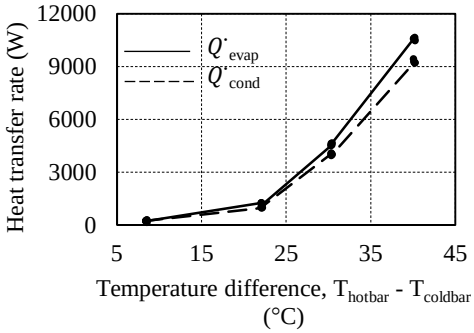

c) $\dot{m}_{air} = 0.841$ kg/s

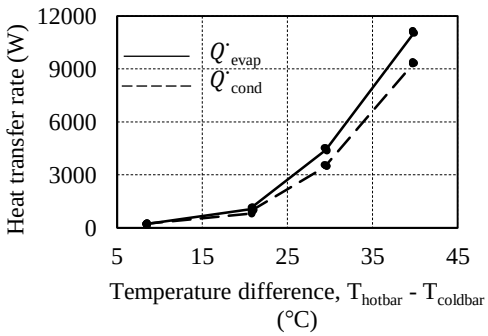

d) $\dot{m}_{air}$ =1.112 kg/s

Figure 18 Thermal resistance curve of the separated-HPHE charged with R123

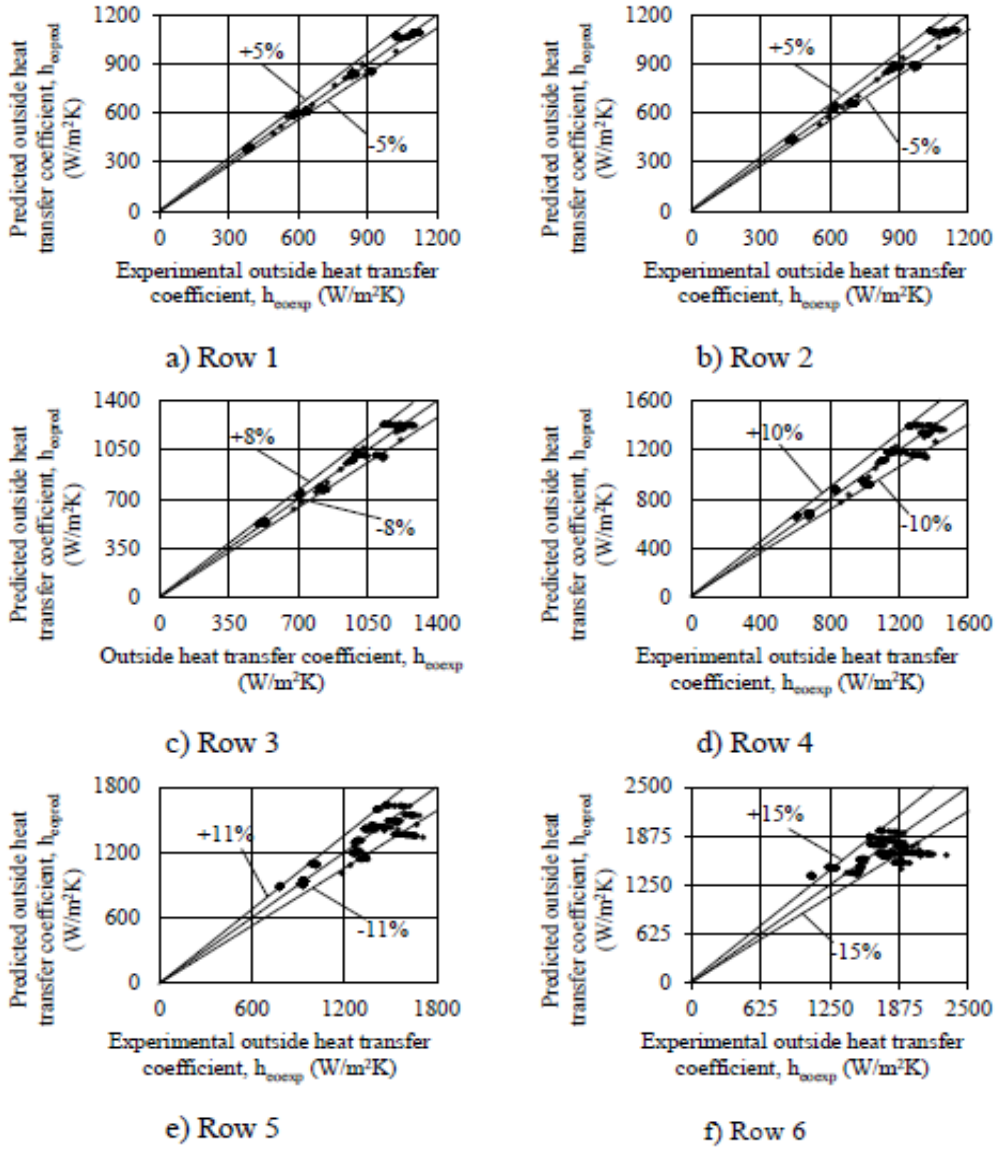

Figure 19 Outside heat transfer coefficients for a geometrically similar HPHE